A New Power Flow Control Approach for Power Converters in Single-phase Microgrids

Sajjad M. Kaviri *, Hadis Hajebrahimi *, Majid Pahlevani **, Praveen Jain *, and Alireza Bakhshai *

* Electrical & Computer Engineering Department,
Queen's University, Kingston, Canada
12ssmk@queensu.ca

** Electrical & Computer Engineering Department,
University of Calgary, Calgary, Canada
majid.pahlevani@ucalgary.ca

***Abstract*— This paper presents a novel control technique for power converters used in single-phase Microgrids (MGs). The proposed control scheme can control the voltage and frequency of the MG while regulating the DC-bus voltage of the power converter. The proposed controller can significantly improve the transient performance of the system while providing a very fast and accurate MG parameters regulation and power sharing. The superior transient performance is due to the fact that, the DC-bus dynamics is embedded in the proposed control system, which enhances the control of input and output parameters (e.g., voltage, frequency, power, etc.). The simulation and experimental results confirm the superior performance of the proposed controller in regulating various parameters in comparison with the conventional proposed droop-based controllers.**

Keywords*— *AC Microgrid, Droop-based Power Sharing, Adaptive Droop Controller, DC-bus Voltage Dynamic, Power Electronic Inverters.

I. INTRODUCTION

The importance of harvesting energy from Renewable Energy Sources (RESs) is undeniable in the future smart grids due to environmental and sustainability concerns associated with the conventional energy sources [1]. In order to achieve the maximum energy harvesting as well as ensure the reliable operation of the smart grids, the concept of Microgrid (MG) has been introduced as the building block of future grids [2]. In MGs, the power electronic converters are the main interface to connect RESs to the grid [1]-[2]. Commonly, typical converters in MGs include an input stage and an output stage. In these converters, the DC-bus capacitor acts as an energy storage interface to connect the two stages together [3]. While the input stage is responsible for extracting the maximum power from RESs, the output stage regulates the DC-bus voltage and shapes the output current [4]-[5].

In power electronic converters the control system plays a key role to enable the MG to achieve its assigned tasks in both of grid-connected and islanded operating modes [6]. The control system is essential in order to ensure the reliable and efficient operation of MGs, as well as control the flow of power between converters and MGs, which can be done through converters [6]-[9]. Various control methods presented to address MG concerns can be classified into two general categories: 1- Centralized methods which are based on communication links and 2- Decentralized methods, which utilize droop controllers and local compensation methods [8],[10]-[12]. Unlike communication-based methods (e.g., centralized, master and slave and etc.) the droop-based methods are not dependent on communication links, which makes them more practical for MG applications [8]-[9]. Despite the advantages of the droop-based methods, their high dependency on grid impedance and inherent trade off between accurate power-sharing and MG parameters regulation are the main drawbacks that should be taken in to account in designing a droop-based MG control system [7]-[9]. While the control of MG parameters (e.g, voltage and frequency) through converters have been addressed in the literature, in most of the proposed methods the dynamics of the DC-bus voltage has been ignored (usually it is considered as an infinite bus with constant voltage) [13]-[14]. However, in practical cases, the dynamics of the DC-bus voltage plays a crucial role in transferring power from the RES to MG, especially in single-phase MGs where the DC-bus voltage control is challenging due to the existence of double frequency ripples in DC-bus voltage [11]-[16]. On the other hand, the regulation of DC-bus voltage is addressed in [3]-[5], [17], while the regulation of MG parameters is not considered in these methods, which make them incompatible with MG requirements in islanded mode. Therefore, most of the presented DC-bus controllers are either so sluggish to be able to use through islanded MGs or do not provide the ability to regulate MG parameters, which is essentials in islanded MGs.

In order to address the mentioned drawbacks of the proposed methods, this paper proposes a novel control scheme for converters used in MGs to control the voltage/frequency at the output stage converter while regulating the DC-bus voltage. The proposed control approach can effectively enhance the transient behavior of the converter by introducing a new DC-bus voltage controller in the closed-loop control system. The proposed controller is based on the singular perturbation control theory. This theory allows the system dynamics to be divided into two manifolds (i.e., slow manifold and fast manifold). Therefore, the controllers for different variables can be designed on these manifolds. In addition, the optimum steady-state value of DC-bus has been derived and utilized to ensure the optimal performance of the two-stage converter during the steady state operating mode. It is being approved that the internal connection between AC-side and DC-bus voltage controllers can significantly improve the transient performance of the proposed controller. In addition, it can regulate the DC-bus voltage variations in the desired range during transients and ensure the optimal performance of the converter.

The rest of this paper is organized as follows: the system description used in this paper to implement the proposed

controller is presented in section II, section III presents the proposed control scheme including adaptive droop controllers for AC-side and DC-bus, DC-bus voltage dynamic analyzer, and the DC-bus voltage optimizer, section IV provides the simulation and experimental results of the implementation of the proposed control scheme, and section V presents the conclusion.

II. System Description

Fig. 1 shows the configuration of a typical medium-scale residential MG used to implement the proposed control scheme. According to Fig. 1, the MG includes RESs including the solar and wind sources with 2.3 and 7kW power ratings, respectively, An energy storage system (3.3 kW power rating), and An RLC load with 8 kVA maximum power demand. RLC load is implemented to cover the different variety of residential loads (i.e. thermal load, fan load, and condensers). All sources are connected to the point of common coupling (PCC) using the two stages power electronic interfaces. In addition, all DG units are equipped with ZigBee modules to provide the low bandwidth communication network between units. According to Fig. 1 it is assumed that the line impedances are negligible in comparison with the RLC load values, which is an acceptable assumption in single-phase islanded MGs [18]-[19].

III. Proposed Control System to Control the Flow of Power in Islanded Microgrids

The general diagram of the proposed control scheme is shown in Fig. 2. According to Fig. 2, the proposed control scheme uses the state-of-the-art structure (i.e. voltage/frequency and DC-bus adaptive droops, a primary controller, and an input stage controller). As can be seen in Fig. 2, The proposed control scheme consists of two control levels: 1- the lower level or converter controller, and 2- the higher level controllers, indicated by yellow background, that provide required references of the lower level controllers. The lower level control system consists of a primary controller (i.e. a power controller along with a current controller to enable the converter to control the flow of power between MG and the converter) and an input stage controller including the MPPT controller to ensure the maximum power harvesting from the DG unit. Base on the proposed control scheme the high level uses a dynamic analyzer and a voltage optimizer to ensure the reliable and optimal performance of the controller during its transient and steady-state performance. The main novelty of the proposed control system lies in the fact that it can highly enhance the transient performance using the dynamic analyzer block and the integrated voltage/frequency and DC-bus adaptive droop controllers.

In conventional methods, the voltage/frequency and DC side droops perform separately, while in the proposed method, they are combined and share the droop gains. This can significantly improve the transient performance of the system. In addition, in conventional control systems, the DC-bus voltage is controlled independently from other controllers. However, in the proposed method the dynamic analyzer adjusts the DC-bus voltage controller gain based on the input power as well as the output load. This gives rise to predictability for the DC-bus voltage, leading to substantially improved the transient response of the system. In addition, the voltage optimizer block

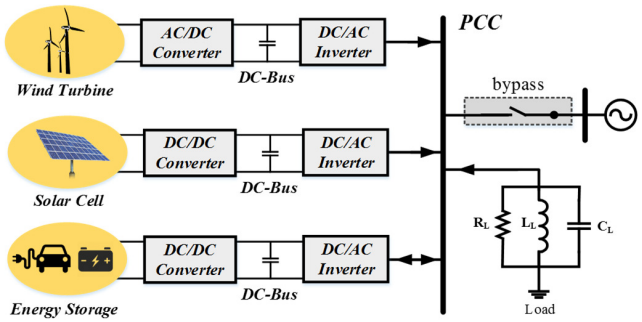

Fig. 1. Configuration of the implemented MG

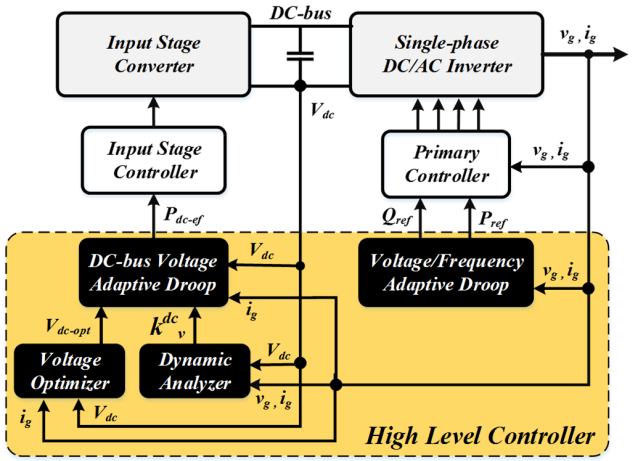

Fig. 2. The proposed Control system general diagram

provides the optimal value for the DC bus voltage during the steady-state operation of the converter. In the following, the procedure to design each of the higher-level control blocks have been investigated.

A. Proposed Adaptive Droop Controllers

Due to the resistive nature of single-phase MGs, the *P/V, Q/ω* droops have been used to achieve a more accurate power-sharing instead of the conventional *P/ω, Q/V* droops [4]. In addition, the proposed control system employs an additional droop controller for the DC-bus voltage, which is crucial to improving the transient performance. Therefore, the proposed control scheme offers three adaptive *P/V, Q/ω* and DC-bus voltage controllers for the single-phase islanded MG to regulate the voltage and frequency of the output bus and DC-bus simultaneously. Moreover, to identify the load changes an impedance estimator along with a network identification algorithm has been used to estimate the load impedance [19].

The main idea of the proposed controller is shown in Fig. 3. According to Fig. 3 in the proposed control system, the voltage/frequency droop controllers provide the active/reactive power references for the primary controller. The active power references for the input-stage controller has also been provided by the DC-bus voltage adaptive droop. The main contribution of the proposed adaptive droops controllers is that the grid voltage droop gains are determined using the DC-bus voltage controller and the DC-bus voltage droop gain is derived using the grid voltage droop controller. This effectively connects the

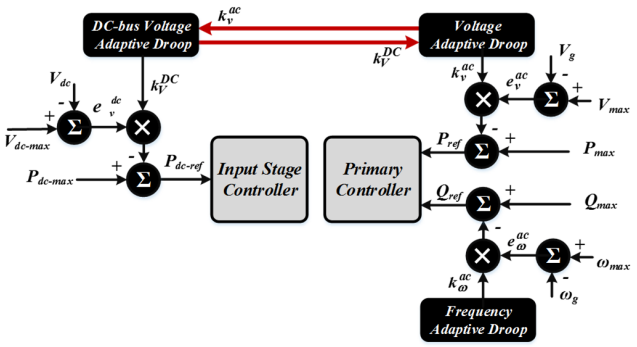

Fig. 3. Proposed adaptive droops control structure

DC-side and AC-side controllers, which can significantly improve the transient performance the control system.

Fig. 4 (a)-(c) show the main idea of the proposed adaptive droop controllers and their derived load and droop profiles. According to Fig. 4, unlike the conventional droop controllers, the proposed controller can regulate voltage/frequency while providing accurate power-sharing by changing the droop slope adaptively based on the load and grid information. According to Fig. 4, to maintain regulated control parameters, the proposed droops profiles (i.e. P^{ac}, Q^{ac}, and P^{dc}) can be derived as:

$$\begin{aligned} P_{ref}^{ac} &= P_{\max} - k_V^{ac}\left(e_V^{ac}\right), \text{ and } e_V^{ac} = V_{\max}^{ac} - V_g \\ Q_{ref}^{ac} &= Q_{\max}^{ac} - \left(k_{\omega L}^{ac} + k_{\omega C}^{ac}\right)\left(e_\omega^{ac}\right), \text{and } e_\omega^{ac} = \omega_{\max}^{ac} - \omega_g \\ P_{ref}^{dc} &= P_{\max} - k_V^{dc}\left(e_V^{dc}\right), \text{ and } e_V^{dc} = V_{\max}^{dc} - V_{dc} \end{aligned} \quad (1)$$

where k_V^{ac}, k_V^{dc}, and k_ω^{ac} are the droop gains and V_g, V_{dc}, and ω_g are the grid voltage amplitude, the DC-bus voltage, and the grid frequency respectively. To integrate the AC and DC-bus voltage controllers, the grid-side and DC-side load profiles can be derived from a combination of loads and droop profiles at AC-side and DC-side as:

$$\begin{aligned} P_{load}^{ac} &= P_{\max} - k_V^{dc}\left(V_{\max}^{dc} - \frac{\left(V_{\max}^{ac} - e_V^{ac}\right)^2}{n_i R_L \mathrm{I_{dc}}}\right) \\ P_{load}^{dc} &= P_{\max} - k_V^{ac}\left(V_{\max}^{ac} - \frac{2I_{dc}}{I_g}\left(V_{\max}^{dc} - e_V^{dc}\right)\right) \\ Q_{Load}^{ac} &= \frac{(V_g)^2}{n_i L_L\left(\omega_{\max}^{ac} - e_\omega^{ac}\right)} - (V_g)^2 \frac{C_L}{n_i}\left(\omega_{\max}^{ac} - e_\omega^{ac}\right) \end{aligned} \quad (2)$$

where R_L, L_L and C_L are the estimated load impedances and I_{dc}, I_g are the magnitude of DC and AC output current and n_i is the initial contributing factor of the ith converter. According to Fig. 4, the intersection of the load and droop profile defines the operating point. Therefore, using intersection of (1) and (2)

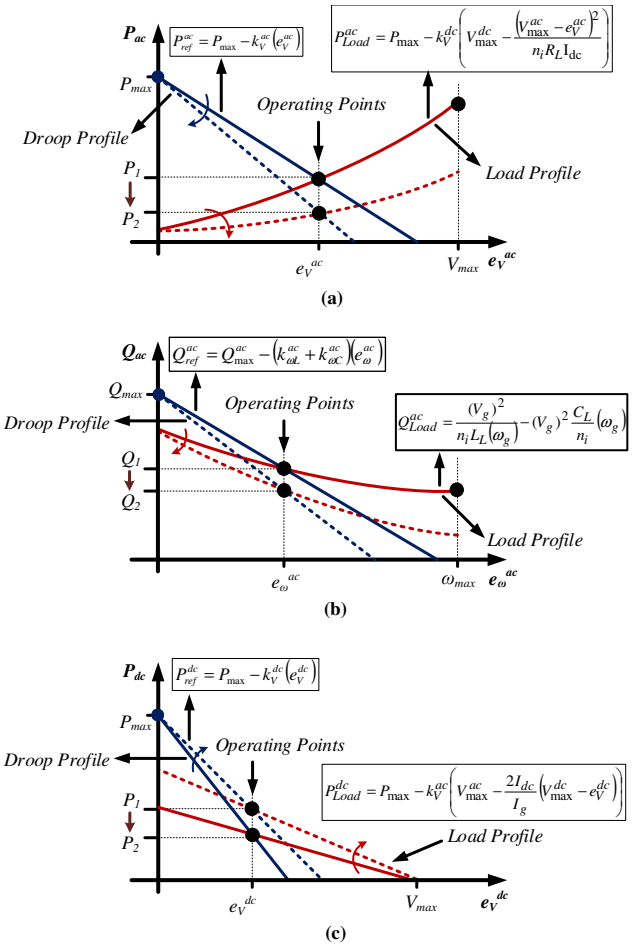

Fig. 4. Proposed adaptive droops curves including (a) grid-voltage, (b) frequency, and (c) DC-bus voltage controllers

and constant error values (e_V^{ac}, e_V^{dc} and e_ω^{ac}) the adaptive droop slopes can be derived as:

$$k_V^{dc} = \frac{V_{\max}^{ac} k_V^{ac}}{e_V^{dc}} - \frac{2V_{\max}^{dc} I_{dc} k_V^{ac}}{I_g e_V^{dc}} + \frac{2I_{dc} k_V^{ac}}{I_g} \quad (3)$$

$$k_{\omega L}^{ac} = \frac{Q_{\max}^{ac}}{e_\omega^{ac}} + \frac{(V_g)^2}{n_i L_L \omega_g e_\omega^{ac}}, \text{ and} \quad (4)$$

$$k_{\omega C}^{ac} = \frac{Q_{\max}^{ac}}{e_\omega^{ac}} + \frac{(V_g)^2 C_L \omega_g}{n_i e_\omega^{ac}}$$

$$k_V^{ac} = \frac{V_{\max}^{dc} k_V^{dc}}{e_V^{ac}} - \frac{\left(V_{\max}^{ac} - e_V^{ac}\right)^2 k_V^{dc}}{n_i R_L I_{dc} e_V^{ac}} \quad (5)$$

In order to guaranty the intersection of the load and droop profiles and have a stable operating point, some conditions should be satisfied as well [20]. According to (3)-(5), the droop slopes can change adaptively based on the variation of load and DG output powers to regulate the voltage/frequency at AC-side

and DC-bus voltage simultaneously. In addition, the integration of AC and DC-bus voltage controllers can significantly improve the transient performance of the system and every change can immediately reflect on the other side controller to ensure a very fast and stable performance.

B. DC-bus Voltage Dynamic Analyzer

One of the prominent features of the proposed controller is its ability to enhance the transient response of the closed-loop control system through the Dynamic Analyzer block. The main objective of the dynamic analyzer block is to determine the droop gain for the DC-bus voltage controller in real-time. The singular perturbation control theory [21] is used to generate the DC-bus droop gain in this block. This theory provides a tool to analyze systems that are included dynamic states with a different rate of changes. The dynamic of the input stage converter, which is typically a DC/DC converter, is so fast due to its very high switching frequency. Therefore the $dI_{dc}/dt >> 0$ and the dynamic of I_{dc} is so faster in comparison with V_{dc} and i_g dynamics and the I_{dc} dynamic is not considered in this paper. Therefore, according to Fig. 5, for the implemented system, the rate of change for the grid current and the DC-bus voltage is given by:

$$\frac{dv_{dc}}{dt} = \frac{1}{C_{dc}} I_{dc} - \frac{1}{C_{dc}} i_g (2d-1) \tag{6}$$

$$\frac{di_g}{dt} = \frac{1}{L_o} v_{dc} (2d-1) - \frac{1}{L_o} V_g \tag{7}$$

Where L_o and C_{dc} are the output inductor and DC-bus capacitor values and d is the duty cycle generated by closed loop control system. According to (6)-(7), the rate of changes for grid current (i_g) is faster than the rate of changes of DC-bus voltage (v_{dc}). Fig. 6 shows the slow and fast dynamic states of the control system. According to Fig. 6, based on Tikhonov's theorem the fast trajectory (i_g) is reached its final steady-state value and can be considered as a constant in the slow trajectory dynamic equation. Therefore, two separate dynamic states can simulate the dynamic behavior of the DC-bus in the variation of i_g and I_{dc}. Therefore, Based on Tikhonov's theorem [22]-[23], the system dynamics can be divided into slow (v_{dc}) and fast (i_g) states if some conditions are satisfied. The main condition of Tikhonov's theorem is the stability of the fast state (i_g). Ones the conditions were satisfied, based on Tikhonov's theorem, the fast state can be considered constant in the slow state dynamic equation as it is already reached its final steady-state values. Thus, the equation (6) can be rewritten as:

$$\frac{dv_{dc}}{dt} = \frac{1}{C_{dc}} I_{dc} - \frac{1}{C_{dc}} i_g^{Cons\tan t}(u), \text{ where}: u = \beta \times k_v^{dc} \tag{8}$$

Therefore to control the dynamic performance of the DC-bus, the droop gain can be rewritten as: $k_V'^{dc} = \beta \times k_V^{dc}$. Where

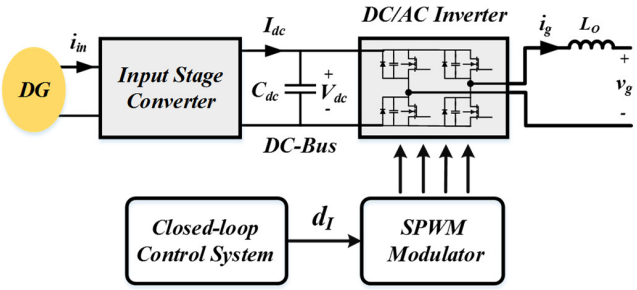

Fig. 5. General configuration of a two-stage converter

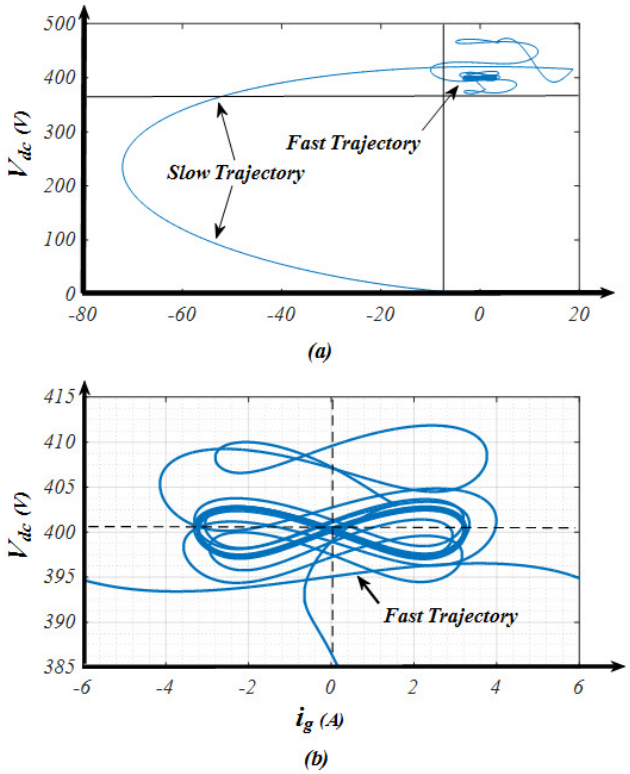

Fig. 6. (a) the Dynamic States of the Control System, (b) detail of the fast state variations

k_V^{dc} is the droop gain generated by adaptive droop and β is the dynamic coefficient to control the DC-bus restoration speed to keep the DC-bus voltage variations in a pre-defined range.

C. DC-bus steady state voltage optimization

One of the main sources of losses in converters is the grid-side output inductor. The amount of losses in this inductor can be controlled by controlling the amount of current ripples flowing through the inductor. Current ripples can be controlled by changing the difference between the DC-bus voltage and the AC-side voltage (V_g). Thus by changing the DC-bus voltage the amount of losses can be reduced greatly. The inductor losses are a combination of the low-frequency losses, that cannot be controlled as it is a function of the output current, and the controllable high-frequency losses as:

$$\Delta L_{Losses} = R_{LF}\left(\Delta I_g\right)^2 + R_{HF}\left(\Delta I_{ripple}\right)^2 + k_C\left(\Delta I_{ripple}\left(\frac{1}{A_C F_s}\right)\right)^{\beta} A_C l_C, \text{ where : } \Delta I_{ripple} = \frac{\left(V_{dc} - V_g\right)d}{L_O F_S} \quad (9)$$

where R_{LF}, R_{HF} are the low and high-frequency resistors of inductor core, d, F_S and L_O are the duty cycle, switching frequency, and output inductor values, and k_C, A_C, l_C and β are the core manufacturer data that are used to calculate the core losses. According to (9), the last two parts present the low-frequency losses that can be reduced by reducing the current ripple which is a function of DC-bus voltage. Considering the voltage drop of the output inductor and DC-bus double frequency ripples, the optimal DC-bus voltage can be derived by minimizing the LF losses as:

$$V_{dc}^{optimal} = \frac{1}{2}\left(\sqrt{\left(V_{\max}^{ac}\right)^2 + I_g^2 L_O^2 \omega_L^2} + \sqrt{\frac{\left((V_{\max}^{ac})^2 C_{dc}\omega_L + \mathrm{I}_g^2 L_O^2 \omega_L^2 C_{dc} + I_g V_{\max}^{ac}\right)}{C_{dc}\omega_L}}\right) \quad (10)$$

Equation (10) presents an optimal DC-bus voltage curve for each value of the output current (I_g). Using (10) the DC-bus voltage reference for DC-bus adaptive droop controller can be adjusted for different output power levels to ensure the optimal performance of the converter in all operating range.

IV. Simulation and Experimental Results

In order to evaluate the proposed control system, the simulation and experimental results are presented in this section. The implemented MG consists of three DGs including a 7kW wind turbine, 2.2 kW solar cell and 3.5 kW storage system. The controller constant errors are set to regulate the MG voltage at 246 V and frequency at 60 Hz. The DC-bus voltages are all regulated at the fixed value of 400 V. The optimal values of DC-bus voltage are not utilized in this session to verify the ability of the proposed controller to regulate the voltage at a fixed value.

Fig. 7 (a) depicts the load profile of the MG. According to Fig. 7 (a), two step-changes have been accrued in active and reactive load power demand at t=0.5 sec and t=1 sec respectively. Fig. 7 (b)-(c) shows the failure of the conventional droops in the regulation of MG voltage/frequency in load variations. Based on these figures the conventional droop-based methods cannot offer the regulation of voltage/frequency in case of load variations, which is crucial for sensitive loads. Fig. 7 (d)-(f) prove the ability of the proposed control to regulate voltage/frequency of MG and DC-bus voltage (Fig. 7 (f)) at the same time. As can be seen the proposed controller can significantly improve the transient performance of the system while offering the regulated MG parameters and DC-bus voltage with low variations, which can guaranty the optimum performance of the islanded MG under load variations.

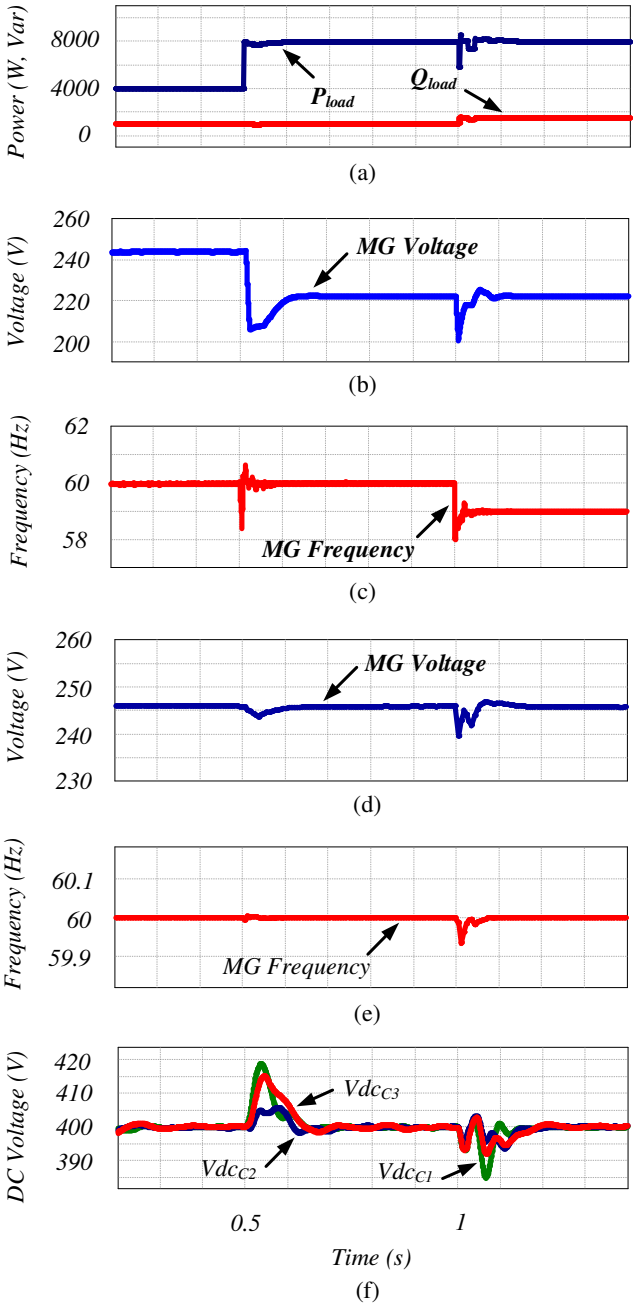

Fig. 7. (a) load profile of MG, conventional droop performance in regulating MG voltage (b) and frequency (c), Proposed controller performance in regulating: (a) MG voltage, (b) MG frequency, (c) DC-bus voltage, and sharing (d) active power, and (e) reactive power

Fig. 8 (a)-(b) illustrate the power-sharing accuracy between parallel converters using the proposed method. According to these figures, the variation of load powers can be accurately shared by parallel converters to keep the MG voltage/frequency constant. It should be noted that based on the implemented control method, the power has been shared between parallel converters based on their ratings, their available power and the dynamic of their DC-bus voltage.

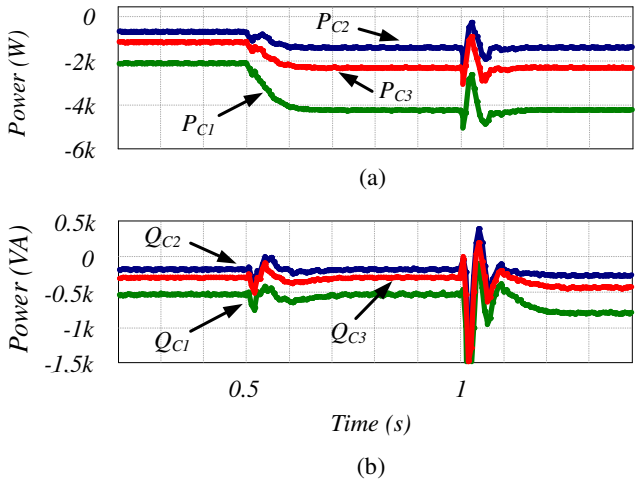

Fig. 8. Proposed controller performance in sharing (a) active power, and (b) reactive power

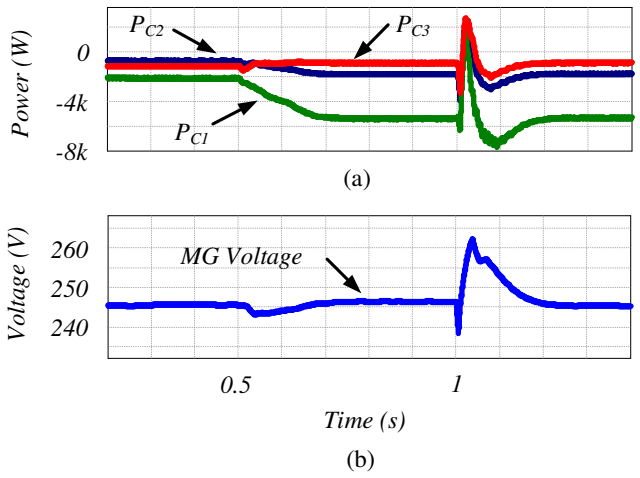

Fig. 9. Proposed controller performance in (a) sharing power and (b) voltage regulation in case of power shortages at DG output

Fig. 9 (a)-(b) shows the ability of the proposed controller to address the power shortages at DC-side. To prove the ability of the controller in the worst case, it is assumed that in t=0.5, when the load demand has been doubled, an input power shortage from DG side has been accrued that force the converter 2 to decrease its output power. According to these figures, the connection between AC and DC-side controllers could decrease the AC-side output to regulate the DC-bus voltage and keep its dynamic changes in a pre-defined range. According to Fig. 9. (b) because of the failure of the second converter to increase its power the MG voltage drops for a limited time which is sensed by other converters and the extra power have been shared between the two other converters based on their ratings to restore the MG voltage at its constant value. According to Fig. 8 and Fig. 9 the proposed method could provide a tightly regulated voltage and frequency in both changes of load demanded power and DG available power while keeping the DC-bus voltage at an optimum level of variations to ensure the optimum performance of the MG and power converters. These figures prove the ability of the presented controller to guaranty the optimum and reliable operation of an islanded MG in all operating conditions.

Fig. 10 illustrate the performance of the DC-bus dynamic analyzer in keeping the DC-bus voltage in a pre-defined range. As can be seen in Fig. 10 in comparison with the simple DC-bus voltage droop controller (the adaptive DC-bus voltage droop without dynamic compensation), the dynamic analyzer block can significantly improve the transient performance of the proposed controller and regulate the DC-bus voltage very fast and with low variation.

An experimental setup including a wind (4kW), a solar (1.5kW), an energy storage (2.5kW) unit, and a 2kW resistive load have been implemented in this paper to prove the ability of the proposed controller to regulate the MG parameters as well as the DC-bus voltage simultaneously. Fig. 11 shows the ability of the controller in power-sharing and MG voltage regulation when the MG load increases from 1 to 2 kW. As can be seen in Fig. 11 the extra demanded power could be successfully shared

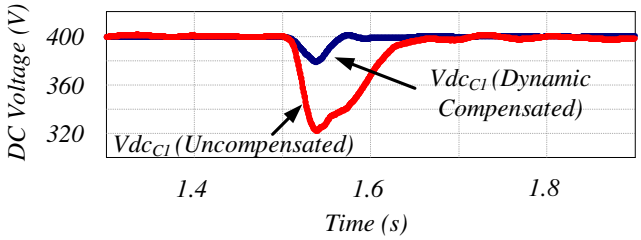

Fig. 10. Performance of dynamic analyzer in limiting the DC-bus voltage fluctuations in case of input/output power variations

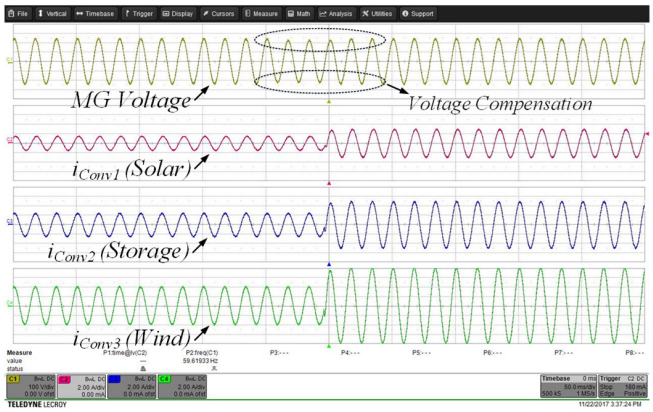

Fig. 11. Transient response of the experimental setup in MG voltage regulation when the proposed control method has been implemented to share the power between parallel converters as well as regulate the MG voltage

between parallel unite based on their power ratings. This leads to the very fast regulation of MG voltage after each load changes. Fig. 12 prove the very fast and robust performance of the DC-bus controller in regulating DC-bus voltage in case of AC side power variations. Based on the Fig. 12 the internal connection of the AC-side and DC-bus voltage controllers can significantly improve the transient performance of the proposed controller.

Fig. 13 prove the ability of the proposed controller to address the power shortages at DC-side. The same load power profile, used in Fig. 12, has been used in this case while a power shortage has occurred for wind unit. As can be seen in Fig. 13 and based on Fig. 12, the wind unit could increase its output power to 5A which is lower than the required power (8A). Therefore, a temporary voltage drop has occurred in MG which is sensed by other converters and they could restore the MG voltage by proving the extra power to compensate the power shortage. Fig. 14 depicts the process of power shortage compensation in more details. Based on Fig. 14 the other two converters, solar and storage, could successfully increase their output power to cover the power shortage happened for wind unit. Based on Fig. 13-14 even in case of power shortages, the proposed control scheme could provide a very fast and reliable voltage regulation inside MG.

V. Conclusion

This paper presents a novel controller for single-phase MG applications to regulate MG parameters and the DC-side voltage at the same time. Unlike previous works, the dynamic of DC-bus has been embedded in the proposed controller to improve the dynamic performance of the system during transients. The integration of the grid-side and DC-bus voltage controller enables the proposed scheme to offer an immediate response during transients while regulating MG voltage/frequency and DC-bus voltage simultaneously. Simulation and experimental results prove the superior performance of the proposed controller in comparison with conventional droop controllers.

References

[1] F. Blaabjerg, Zhe Chen and S. B. Kjaer, "Power electronics as efficient interface in dispersed power generation systems," in *IEEE Transactions on Power Electronics*, vol. 19, no. 5, pp. 1184-1194, Sept. 2004.

[2] D. E. Olivares, A. Mehrizi-Sani, A. H. Etemadi, C. A. Canizares, R. Iravani, M. Kazerani, A. H. Hajimiragha, O. Gomis-Bellmunt, M. Saeedifard, R. Palma-Behnke, and N. D. Hatziargyriou, "Trends in Microgrid control," *IEEE Transactions on Smart Grid*, vol. 5, no. 4, pp. 1905–1919, Jul. 2014.

[3] S. Eren, M. Pahlevani, A. Bakhshai and P. Jain, "An Adaptive Droop DC-Bus Voltage Controller for a Grid-Connected Voltage Source Inverter With LCL Filter," in *IEEE Transactions on Power Electronics*, vol. 30, no. 2, pp. 547-560, Feb. 2015.

[4] T. L. Vandoorn, B. Meersman, L. Degroote, B. Renders and L. Vandevelde, "A Control Strategy for Islanded Microgrids With DC-Link Voltage Control," in *IEEE Transactions on Power Delivery*, vol. 26, no. 2, pp. 703-713, April 2011.

[5] M. Pahlevani and P. Jain, "A Fast DC-Bus Voltage Controller for Bidirectional Single-Phase AC/DC Converters," in *IEEE Transactions on Power Electronics*, vol. 30, no. 8, pp. 4536-4547, Aug. 2015.

[6] J. M. Guerrero, M. Chandorkar, T. L. Lee and P. C. Loh, "Advanced Control Architectures for Intelligent Microgrids—Part I: Decentralized and Hierarchical Control," in *IEEE Transactions on Industrial Electronics*, vol. 60, no. 4, pp. 1254-1262, April 2013.

[7] J. M. Guerrero, J. C. Vasquez, J. Matas, L. G. de Vicuna and M. Castilla, "Hierarchical Control of Droop-Controlled AC and DC Microgrids—A General Approach Toward Standardization," in *IEEE Transactions on Industrial Electronics*, vol. 58, no. 1, pp. 158-172, Jan. 2011.

[8] H. Han, X. Hou, J. Yang, J. Wu, M. Su and J. M. Guerrero, "Review of Power Sharing Control Strategies for Islanding Operation of AC Microgrids," in *IEEE Transactions on Smart Grid*, vol. 7, no. 1, pp. 200-215, Jan. 2016.

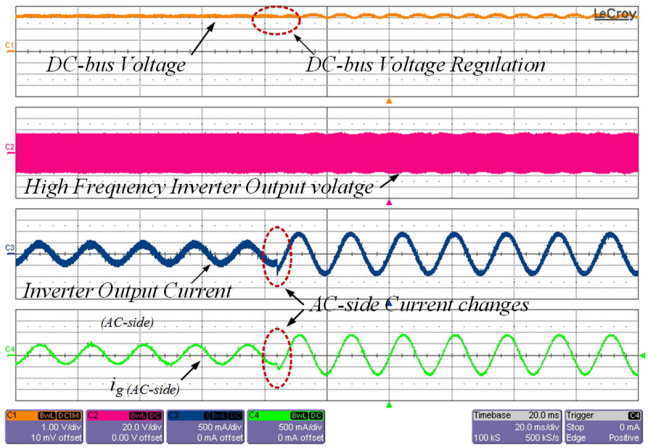

Fig. 12. Transient response of the experimental setup in DC-bus voltage regulation in case of AC-side current variations (the results are captured using X10 probes)

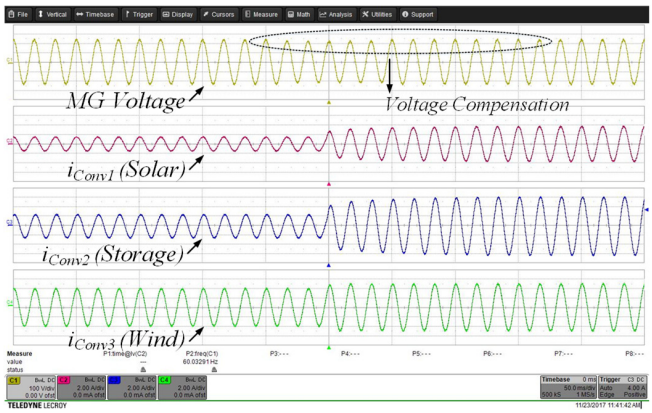

Fig. 13. Transient response of the experimental setup in MG voltage regulation in case of power shortage at wind source (Converter 3)

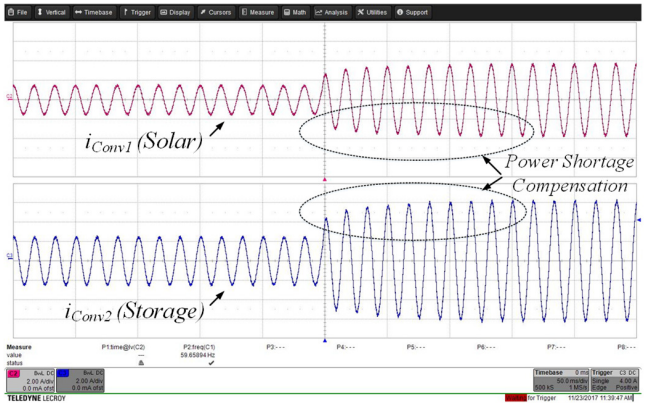

Fig. 14. Transient response of the experimental setup in current sharing in case of power shortage at wind source (Converter 3)

[9] Y. Han, H. Li, P. Shen, E. A. A. Coelho and J. M. Guerrero, "Review of Active and Reactive Power Sharing Strategies in Hierarchical Controlled Microgrids," in *IEEE Transactions on Power Electronics*, vol. 32, no. 3, pp. 2427-2451, March 2017.

[10] J. A. P. Lopes, C. L. Moreira, and A. G. Madureira, “Defining control strategies for microgrids islanded operation,” *IEEE Transactions on Power Systems*., vol. 21, no. 2, 2006.

[11] F. Blaabjerg, R. Teodorescu, M. Liserre and A. V. Timbus, "Overview of Control and Grid Synchronization for Distributed Power Generation Systems," in *IEEE Transactions on Industrial Electronics*, vol. 53, no. 5, pp. 1398-1409, Oct. 2006.

[12] S. M. Kaviri, M. Pahlevani, P. Jain and A. Bakhshai, "A review of AC microgrid control methods," *2017 IEEE 8th International Symposium on Power Electronics for Distributed Generation Systems (PEDG)*, Florianopolis, 2017, pp. 1-8.

[13] Q. Shafiee, J. M. Guerrero, and J. C. Vasquez, “Distributed secondary control for Islanded Microgrids—A novel approach,” *IEEE Transactions on Power Electronics*, vol. 29, no. 2, pp. 1018–1031, Feb. 2014.

[14] T. L. Vandoorn, J. D. M. De Kooning, and B. Meersman, “Review of primary control strategies for islanded microgrids with power-electronic interfaces,” *Renew. Sustain. Energy Rev.*, vol. 19, pp. 613–628, Mar. 2013.

[15] S. M. Kaviri, T. A. Najafabadi, B. Mohammadpour, P. Jain and A. Bakhshai, "Modified window, recursive least square estimator for active and reactive powers in single-phase AC systems," *2016 IEEE 7th International Symposium on Power Electronics for Distributed Generation Systems (PEDG)*, Vancouver, BC, 2016, pp. 1-6.

[16] S. M. Kaviri, M. Pahlevani, B. Mohammadpour, P. Jain and A. Bakhshai, "Power control of a bi-directional AC/DC rectifier used for telecom backup systems," *2015 IEEE International Telecommunications Energy Conference (INTELEC)*, Osaka, 2015, pp. 1-5.

[17] S. M. Kaviri, M. Pahlevani, B. Mohammadpour, P. Jain and A. Bakhshai, "A D-Q rotating frame DC-bus voltage controller for bi-directional single-phase AC/DC converters," *2015 IEEE Energy Conversion Congress and Exposition (ECCE)*, Montreal, QC, 2015, pp. 3468-3473.

[18] J. C. Vasquez, J. M. Guerrero, A. Luna, P. Rodriguez, and R. Teodorescu, “Adaptive droop control applied to voltage-source Inverters operating in grid-connected and Islanded modes,” *IEEE Transactions on Industrial Electronics*, vol. 56, no. 10, pp. 4088–4096, Oct. 2009.

[19] L. Asiminoaei, R. Teodorescu, F. Blaabjerg and U. Borup, "A digital controlled PV-inverter with grid impedance estimation for ENS detection," in IEEE Transactions on Power Electronics, vol. 20, no. 6, pp. 1480-1490, Nov. 2005.

[20] S. M. Kaviri, H. Hajebrahimi, M. Pahlevani, P. Jain and A. Bakhshai, "A hybrid adaptive droop control technique with embedded DC-bus voltage regulation for single-phase microgrids," *2017 IEEE Energy Conversion Congress and Exposition (ECCE)*, Cincinnati, OH, USA, 2017, pp. 3359-3366.

[21] P. Kokotovic, H. K. Khalil, J. O’Reilly, *Singular Perturbation Methods in Control*, Siam ISBN 0-89871-444-3 1999.

[22] A.N. Tikhonov, S*ystems of differential equations containing a small parameter multiplying the derivative*, Mat. Sb. 31 (1952) pp. 575-586.

[23] F. Verhulst, *Methods and applications of singular perturbations, boundary layers and multiple timescale dynamics*, Springer-Verlag (2005) 340 pp.6.